UDC 620.93
IRSTI 29.31.15

https://doi.org/10.55452/1998-6688-2025-22-4-401-410

[1]Zhukeshov A.M.,
Dr. Phys.-Math. Sc., Professor, ORCID ID: 0000-0001-9153-323X,
e-mail: zhukeshov@physics.kz
[1]*Abdybai U.B.,
PhD student, ORCID ID: 0009-0002-5309-5827,
*e-mail: abdibay_ulan@mail.ru
[1]Salimov E.E.,
PhD student, ORCID ID: 0009-0005-7712-6263,
e-mail: Salimov_ernar@mail.ru
[2]Carlos M.,
Professor, ORCID ID: 0000-0002-7374-505X,
e-mail: Carlos.meza@ieee.org

[1]Al-Farabi Kazakh National University, Almaty, Kazakhstan
[2]The university of applied Sciences of Anhalt, Anhalt, Germany

COMPARATIVE PERFORMANCE CHARACTERISTICS OF METAL-AIR BATTERIES WITH CAST AND POROUS ELECTRODES

Abstract

Currently, the development of electrochemical energy storage systems plays a key role in meeting the growing demand for electric power. Metal-air batteries (MAB) with high specific energy capacity are considered as promising solutions for use in power plants as backup power sources. One of the main limitations of their widespread implementation is the need to improve the efficiency of anode materials. In this paper, we propose the use of porous aluminum electrodes to improve the performance of MAB. Two types of porous anodes manufactured using different technologies were studied. For the powder aluminum anode, the current density was 20–30 mA/cm², which is comparable to the performance of a monolithic (standard) anode. At the same time, foam aluminum demonstrated higher current density values of 52–64 mA/cm². An additional advantage of porous anodes is their reduced weight (by 10–30%), which helps to improve the weight and size characteristics of MAB and opens up opportunities for creating more efficient energy systems.

Keywords: metal–air battery, aluminum anode, porous electrode, aluminum foam, electrochemical performance, specific surface area, energy storage.

Introduction

At the current stage of energy development, the problem of energy storage during periods of sudden decrease in its generation is of particular relevance, which is necessary to ensure a stable quality of power supply and meet increasing demand [1–3]. Among various energy storage technologies, electrochemical systems demonstrate the best compliance with the key requirements of scalable solutions, such as a long service life, high efficiency, and the ability to adapt to different consumption levels. Of particular interest among electrochemical storage devices are metal-air batteries (MAB), which are distinguished by a significantly higher theoretical energy capacity compared to traditional battery systems [4]. However, their practical application is limited by a number of technical problems associated with the design of the metal anode, air cathode, and electrolyte stability [5]. Considering that MAB have the highest potential energy capacity among known types of energy sources, environmentally friendly and affordable metals, such as iron, zinc, and especially aluminum, are considered promising materials for electrodes. Aluminum, in particular, has a high degree of recyclability, significant energy density (8.1 kWh/kg) and electrochemical potential (1.7 V), making it commercially attractive for use in MAB.

The study of metal electrodes in metal-air batteries (MAB) faces a number of technical challenges, including dendrite formation, electrode deformation, corrosion processes, side reactions, and surface passivation [6]. Currently, active attention is paid to anode materials based on zinc, aluminum, and iron. For example, Parker et al. proposed a three-dimensional zinc sponge-type structure with interconnected porosity and high conductivity, which made it possible to effectively suppress the formation of large-scale dendrites [7]. Another study presented a Zn anode with a developed specific surface area obtained by bubble synthesis [8]. It was found that reducing the pore size contributes to an increase in the efficiency of zinc-air batteries. Aluminum anodes are also the subject of intensive research. A series of studies by Wen and colleagues [9–11] showed that alloying aluminum with Mg, Ga, Sn, and Mn metals increases its electrochemical activity compared to pure Al. The study describes a simple method for producing a porous aluminum anode by applying Al powder onto aluminum foil [12]. The resulting powder electrode ensured a decrease in local current density and contributed to uniform deposition of aluminum. It should be noted that there are significantly fewer publications devoted to porous anodes for MAW compared to studies of porous cathodes. The latter are actively being developed using nanomaterials such as nanotubes, graphene, and others [13–16]. However, cathode catalysis is not considered in this paper.

Metal–air batteries (MABs) find applications in both automotive and portable electronics, demonstrating potential for widespread implementation in various technological areas [17–19]. In particular, aluminum–air systems are considered as promising solutions for highly efficient energy storage. However, despite active research, a number of fundamental scientific and engineering problems that limit the commercialization and large-scale implementation of MABs remain unresolved [20–23].

Thus, the key tasks in the development of new electrode materials are to minimize corrosion processes, suppress dendrite formation and improve electrochemical characteristics, including specific capacity. One of the effective approaches to improving the anode properties is to increase the specific surface area of the electrode. Expanding the contact zone between the electrode and the electrolyte promotes an increase in the number of active sites, which in turn reduces the local current density and stabilizes electrochemical processes. Porous materials, having a reduced density, allow reducing the mass of the electrode while maintaining its geometric parameters, which can be useful for optimizing energy characteristics. However, questions related to the behavior of exothermic reactions in such structures, possible local heating of the anode body and the magnitude of the total current remain open. The study of these aspects and the assessment of the practical efficiency of porous anodes under real operating conditions of metal-air batteries is the main goal of this study.

There are several ways to create porous materials. The standard method is to obtain metal foam in a gas flow with various manipulations. Depending on the pore structure, namely open or closed, the metal foam can be multifunctional, which makes it suitable for highly specialized applications [24]. The analysis conducted showed that the porosity of aluminum foam can be in the range from 55 to 70%, and the maximum energy absorption capacity is achieved in a metal foam with a porosity of 57% [25]. Recently, studies have been conducted on the preparation of porous intermetallic compounds containing Al using the combustion synthesis (CS) reaction [26]. The reaction mechanism for the M–Al system (M = Ti, Ni, Fe, Nb, and Cu) is closely related to the state of aluminum (e.g., solid or liquid phase) and largely depends on the processing parameters such as particle size, Al content, heating rate, pressing pressure, sintering temperature, content and type of pore-forming agents. It should also be noted that porous materials are successfully used not only as anodes, but also as cathodes in metal-air batteries. 3D catalyst film made of copper and carbon with a double 3D porous structure was manufactured [27]. The finished composites were used as an air cathode in an aluminum-air battery, which demonstrated good water resistance and air permeability.

Materials and methods

In this work, two types of porous materials were used. The surface appearance of the anodes of the first and second types is shown in Figure 1. A cast electrode (hereinafter referred to as a monolith) of the same size, cut from an A0 aluminum sheet, was used as a comparison (Figure 2). All samples had the same area (20x30x4) mm3.

The first type of samples was obtained by self-fabrication from metal powders. Pressed powder materials used in this process also have a porous structure, which makes them promising for use as anodes. Chemically pure aluminum powder with a particle size of about 30 μm was used to form porous aluminum anodes. The process included the following main stages: preliminary mixing of aluminum powder with 10% copper powder, loading the resulting mixture into a collapsible press mold and subsequent pressing at a force of 12 tons until a dense blank was obtained. Then thermal annealing was carried out in a vacuum electric furnace at a temperature corresponding to the formation of an equilibrium eutectic (about 0.6 of the melting point), followed by cooling until it solidified. As a rule, pressure in the range of 250–400 MPa is used to press aluminum powders. If it is necessary to calculate the force required to press a platform with a given area S at a pressure of 2500–4000 kgf/cm², the following formula is used:

$$F = P \times S\ , \tag{1}$$

Thus, to press disks with a diameter of 2–5 cm at a pressure of 2500–4000 kgf/cm², a force of ~8 to ~79 thousand kg/f is required, which corresponds to approximately 8–79 tons. In the experiment, a force of about 12 tons was used, which corresponds to pressing a disk with a diameter of about 2.5–3 cm at medium pressure.

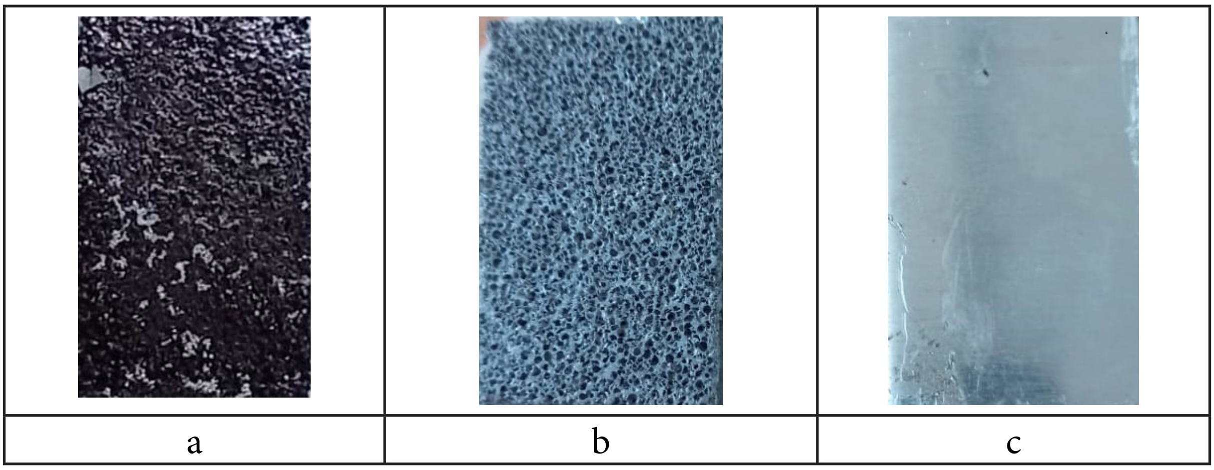
a
b
c

Figure 1 – Samples of porous anodes of type 1 (a) and type 2 (b)
and Cast aluminum anode (c). Sample dimensions 20x30 mm.

Samples of porous anodes of the second type are aluminum foam (hereinafter referred to as foam) obtained by industrial gas spraying (manufacturer - Kunshan New Materials Corp., China). Foam density characteristics are given in Table 1. The key parameters determining the physical and mechanical properties of the foam are its density and porosity, i.e. the volume of pore space. Porosity is calculated using the following formula:

$$\Pi = \left(1 - \frac{\rho_0}{\rho}\right) 100\ , \tag{2}$$

where Π is the porosity in %, ρo is the density of the finished (sintered) material, ρ is the density of the cast material. The density of the foam metal (g/cm^3) was determined in a standard way using the formula: ρo = m/V where m is the mass of the sample, V is the volume of the sample. Traditionally, in the production of foam materials, the main characteristic of porosity is designated PPI - the average number of Pores Per Inch. The data for our material are as follows: PPI = 45, the average pore size is 0.5 mm. Figure 1 b shows the foam surface at an optical magnification of 10X, from which it is clear that the pore sizes are indeed about 500 μm. The free surface area is determined by the pore size and the bulk density of the foam material [28]. The nature of the dependence of these parameters is linear and is presented below by the formula

$$S = k \times (PPI)\ \left[\frac{m^2}{m^3}\right]. \tag{3}$$

For the given PPI value, the specific area is in the range of 2500–3500 m2/m3. Then, according to formula (1), for our foam material, the effective surface area will be Sef = (32000±3000) cm2.

The surface area of the powder material was determined based on the following considerations. Unlike 3D foam, here by the surface area we mean the area of the microscopic relief on the surface formed by the natural roughness due to the structure of the material. If we assume that the powder particles are ideally sintered and form spherical structures, we can assume that the surface is covered with microspheres (more precisely, hemispheres). If we discuss about the effective surface area Sef, we understand that its assessment should be conducted in this study. This parameter cannot be measured directly, but we can model the relative increase in the original (flat) surface area S. The surface relief of aluminum powder compound showed in Figure 2 (a). At the surface level, white particles of sintered aluminum powder with sizes from 60 to 80 μm are visible, located in a matrix of black oxide. The average size of spherical aluminum particles is 70 ±10 μm. 5-10 particles fit on the 1000 μm line. Then the degree of filling of the surface with aluminum particles will be 60%. Let us assume that the roughness of the surface is conventionally sphere-shaped and distributed uniformly over the surface. Then, using the square of the semi-sphere, we can determine the coefficient of increase in the surface area using the following formula:

$$K = \frac{S_{ef}}{S} = \frac{NS_{sph}}{2S_{flat}} \tag{4}$$

Where Ssph and Sflat are the areas of the lateral surface of the spheres and flat base, respectively; N is the number of spheres pleased on the flat square of sample S = ab; If N ~ (ab)*d2

$$K = \frac{ab}{d^2}\frac{\pi d^2}{2ab} = \frac{\pi}{2} \tag{5}$$

According to equation (4), the coefficient K is 1.57. Thus, according to the calculation results, the effective surface area S of the aluminum sample exceeds the nominal area S by 57%. In this case, the calculations assumed that the spherical particles uniformly cover the entire surface. The image shown in Figure 2a visually creates the impression of dark gaps between the spheres. However, this is not true: similar particles are present in these areas, but they are located at a lower level. The uniformity of the surface relief is confirmed by the profilometry data shown in Figure 3a. As can be seen, the vertical profile is an alternation of protrusions and depressions, while the maximum depth of the depressions reaches Rz = 67, which is consistent with the previously obtained microscopic data.

An experimental cell of a metal-air battery (MAB) was developed to test the anodes. A schematic cross-sectional view of the device is shown in Figure 4. The electrolyte (position 1) fills the reaction chamber (2) located between the air cathode (3) and the anode (4). The anode under test was immersed in the electrolyte and fixed at a distance of 2 cm from the cathode surface. An aqueous solution of potassium hydroxide with a concentration in the range of 0.1–1.4 mol/l was used as the electrolyte. The air cathode was made of cardboard based on porous carbon fiber. Current collection was carried out using a metal grid fixed to the cathode using a metal plate.

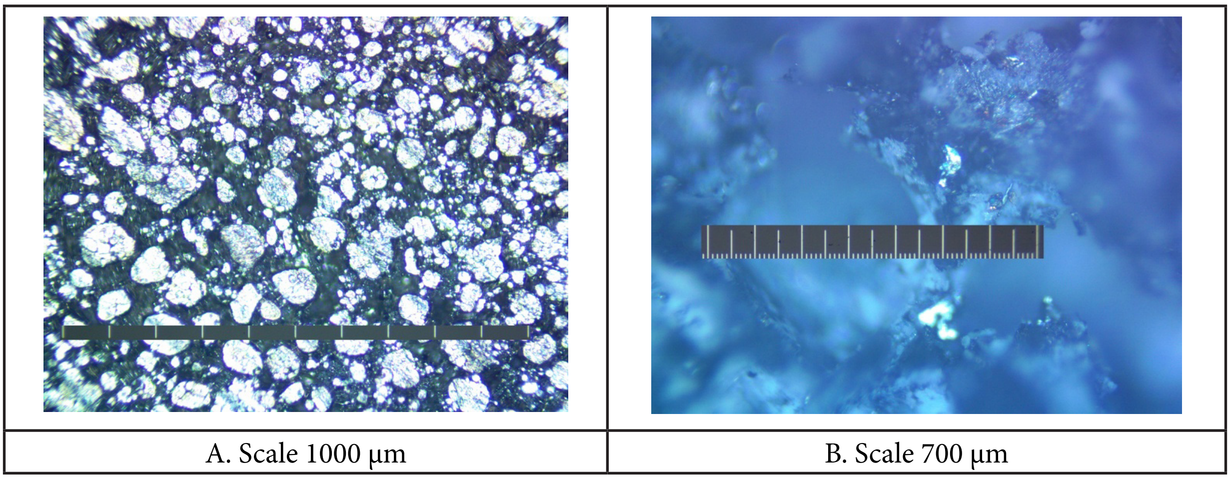
A. Scale 1000 µm
B. Scale 700 µm

Figure 2 – Particles of aluminum powder (a)
and Pores in aluminum foam (b) at 10X optical magnification.

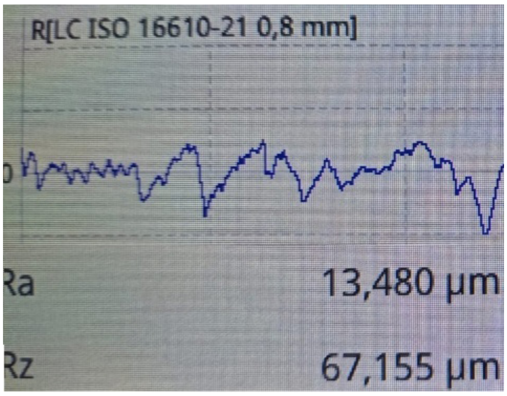
R[LC ISO 16610-21 0,8 mm]

Ra 13,480 µm

Rz 67,155 µm

Figure 3 – Roughness of powder alumina surface

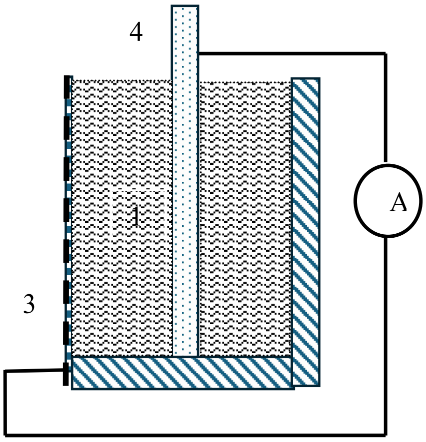

Figure 4 – Elements of the design of the experimental cell MAB for testing anodes

The current was measured using a Fluke 8655 multimeter. Optical images of the surface were taken using a digital camera in macrofocus mode and an AM Scope 580 T microscope. Roughness profile measurements were performed using a device MahrSurf 10S. The device has an induction reference sensor, tip radius 2 µm. The measurement ranges of the roughness parameter are: Ra from 0.02 to 10 µm, Rz, Rmax — from 0.1 to 50 µm. The length of the probing path is 0.56 - 16 mm.

Results and discussion

When powdered aluminum (see Figure 1) interacted with a 1-mol KOH electrolyte, an intense exothermic reaction was observed. During the experiment, the sample significantly lost weight, and white spots characteristic of oxide compounds formed on its surface. Foamed aluminum also demonstrated an active reaction when in contact with the same electrolyte, accompanied by intense gas evolution. In order to preserve the integrity of the three-dimensional structure of the material, it was decided to reduce the alkali concentration to 0.1 mol for subsequent tests. Unlike the above-mentioned samples, the anode made of cast aluminum demonstrated more stable behavior when interacting with a 1-mol electrolyte solution — the oxidation process occurred uniformly and without pronounced turbulence.

Table 1 shows the mass losses of different electrodes after 30 minutes of operation in 1M KOH electrolyte.

Table 1 – Mass loss of different electrodes within 30 min at a concentration of 1 M

Material	Cast aluminum	Aluminum powder	Foam aluminum
Initial mass, g	5.645	6.158	1.640
Final Mass, g	5.592	4.709	1.0145
Density, g/cm3	2.437	1.102	0.683
Specific area, Sef, cm2	12	18.75	33000
Weight loss in 10 min, mg	13	1450	622

The high mass loss coefficient observed in porous materials, especially aluminum foam, is due to their developed specific surface area. This leads to an increase in the area of active reaction, which in turn helps to reduce the current density per unit surface area. The current density was calculated using the following formula:

$$j = \frac{I}{S_{ef}} \ ,$$

where I is the short-circuit current measured by the device in Figure 3, and Sef is the effective surface area of the anode, i.e. the area that is in contact with the electrolyte. To calculate the effective area, we take both sides of the surface of the samples in contact with the electrolyte, both from the cathode side and from the back side. Further in the calculations, we took S = 2ab = 12 cm2.

Taking these considerations into account, the porous anode samples were tested in the MAB electrochemical cell for all types of anodes in electrolytes with a concentration of 0.1 and 4 mol, respectively. Figure 5a shows the time dependences of the short-circuit current I for anodes made of aluminum powder (p), aluminum foam (f), and monolith (s) during testing for 10 min at 0.1 mol. A characteristic feature of the current behavior for all types of samples is an increase in current at the beginning of the experiment, then its saturation and decline over time. This is due to the activation of the entire surface of the sample after the removal of the oxide layer on the surface.

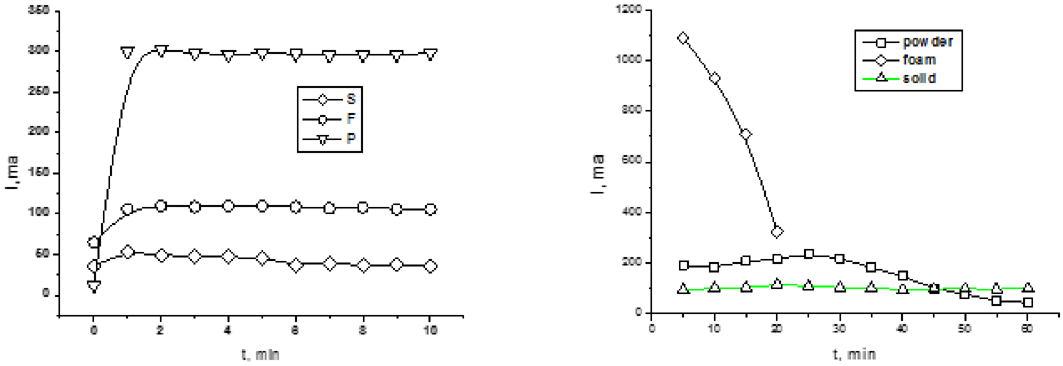

a) b)

Figure 5 – a) Dependence of the anode current on time for monolithic (s) and powder (p) at a concentration of 1 mol/l, b) aluminum foam (f) at a concentration of 0.1 mol/l)

For the anodes of the first type, the highest current density was recorded for the aluminum powder sample, reaching values of j = (25–30) mA/cm². Let us move on to the analysis of the anodes of the second type. The key observation here is that foam aluminum demonstrates a more than twofold excess of current density compared to monolithic aluminum. This is explained by the capillary effect: the electrolyte actively penetrates the porous structure of the material, which significantly increases the effective area of the electrochemical reaction.

According to the measured values of current density:

- for foam aluminum – j = (9–11) mA/cm²
- for the monolith – j = (3–5) mA/cm²

Considering that the electrolyte concentration in this case is only 0.1 mol, it can be assumed that at a standard concentration of 5–6 mol, the current density will increase by an order of magnitude. For comparison, according to literature data, cast aluminum anodes at a concentration of 6 mol demonstrate an average current density of about 50 mA/cm². However, for the first two types of materials, the effective areas of the samples cannot be considered equal, since the foam material, unlike the powder, interacts with the electrolyte not only on the surface, but also in the bulk structure. Taking into account the above formulas (1–4), the current density for the powder anode decreases by 1.57 times, and for foam aluminum – by 32,000 times. As a result, we obtain the following values: 39 mA/cm² for the powder anode and 0.003 mA/cm² for the foam. Thus, an important conclusion is that the powder anode demonstrates a high current density even at an extremely low concentration of the working electrolyte – 0.1 mol/l.

Next, we will consider the data at an electrolyte concentration of 4 mol/l (Figure 5b). In this case, the highest short-circuit current is demonstrated by foam aluminum. The current values exceed 1 A and are not the limit, since in some experiments currents of up to 5 A were recorded at a cell voltage of up to 4 V. However, at a high electrolyte concentration (4 mol/l and higher), the foam quickly loses mass, and after 20 minutes the sample is completely destroyed. Unlike foam, the powder anode shows more stable behavior: in the first 30 minutes, the current increases slightly within 190–220 mA, and then gradually decreases. This is due to a decrease in the anode mass, since the active area is reduced when the lateral surface becomes thinner. The behavior of the monolith remains unchanged, similar to that observed at a concentration of 0.1 mol/l. Taking into account the specific area, the current density for the three materials is: 0.03 mA/cm² for the foam, 26 mA/cm² for the powder, and 8.3 mA/cm² for the monolith. At the same time, the calculations did not take into account the decrease in the surface area and volume of the samples during etching, so the given values reflect the initial stage of the experiment. As a result, at a concentration of 4 mol/l, the current density of the powder anode is again higher than that of the monolith.

Conclusion

Thus, porous materials demonstrate different current densities depending on their manufacturing method. For powder anodes, this value is close to the values of monolithic samples (26–39 mA/cm²), but the high etching rate leads to structural changes, which requires additional study. At the same time, the mass of powder anodes is 10–30% lower, which is an advantage in the context of the mass-dimensional characteristics for MABs.

The foam material showed significantly higher current characteristics compared to powder samples. However, it is important to consider that intense current leads to accelerated destruction of the aluminum foam electrode. Despite this, when developing MABs as energy storage devices, where a sharp increase in current output is required while maintaining the overall mass of the device, this parameter may be critically important.

A notable effect recorded during the experiment was the ability of aluminum foam to draw in electrolyte due to the capillary effect. In the future, this phenomenon can be used to create high-speed MABs that operate without the need for forced injection of electrolyte.

In practical terms, the materials studied here can be considered for use in systems that operate in intermittent or emergency modes, where a fast current response is required. Such metal–air modules may become relevant for small backup power units, portable field electronics and communication sensors that work away from centralized infrastructure. At the same time, the reduced mass of porous anodes opens up the possibility of using them in compact autonomous energy systems, where every additional gram is critical. These aspects outline a realistic direction for further development of the proposed solutions.

The experiments conducted confirm the potential of using porous anodes in the creation of highly efficient autonomous power microsystems (APM).

Information about funding. The work was carried out with the support of grants from the Ministry of Education and Science of the Republic of Kazakhstan. BR21882187 and ИРН AP19676182.

REFERENCES

1 Narayanan, S.R., Prakash, G.K.S., Manohar, A., Yang, B., Malkhandi, S., & Kindler, A. Materials challenges and technical approaches for realizing inexpensive and robust iron–air batteries for large-scale energy storage. Solid State Ionics, 216, 105–109 (2012). https://doi.org/10.1016/j.ssi.2012.05.016.

2 Han, X., Li, X., White, J., Zhong, C., Deng, Y., Hu, W., & Ma, T. Metal–air batteries: From static to flow system. Advanced Energy Materials, 8, 1801396 (2018). https://doi.org/10.1002/aenm.201801396.

3 Fan, X., Liu, B., Liu, J., Ding, J., Han, X., Deng, Y., Lv, X., Xie, Y., Chen, B., Hu, W., et al. Battery technologies for grid-level large-scale electrical energy storage. Transactions of Tianjin University, 26, 92–103 (2020). https://doi.org/10.1007/s12209-019-00236-w.

4 Salameh, T., Sayed, E.T., Abdelkareem, M.A., Olabi, A.G., & Rezk, H. Optimal selection and management of hybrid renewable energy system: Neom city as a case study. Energy Conversion and Management, 244, 114434 (2021). https://doi.org/10.1016/j.enconman.2021.114434.

5 Li, Y., & Lu, J. Metal–air batteries: Will they be the future electrochemical energy storage device of choice? ACS Energy Letters, 2(6), 1370–1377 (2017). https://doi.org/10.1021/acsenergylett.7b00119.

6 Wang, H.F., & Xu, Q. Materials design for rechargeable metal–air batteries. Matter, 1(3), 565–595 (2019). https://doi.org/10.1016/j.matt.2019.05.018.

7 Parker, J.F., Chervin, C.N., Nelson, E.S., Rolison, D.R., & Long, J.W. Wiring zinc in three dimensions rewrites battery performance – dendrite-free cycling. Energy & Environmental Science, 7, 1117–1124 (2014). https://doi.org/10.1039/C3EE43674H.

8 Liu, P., Ling, X., Zhong, C., Deng, Y., Han, X., & Hu, W. Porous zinc anode design for Zn–air chemistry. Frontiers in Chemistry, 7, 656 (2019). https://doi.org/10.3389/fchem.2019.00656.

9 Pino, M., Cuadrado, C., Chacón, J., et al. The electrochemical characteristics of commercial aluminium alloy electrodes for Al–air batteries. Journal of Applied Electrochemistry, 44, 1371–1380 (2014). https://doi.org/10.1007/s10800-014-0739-4.

10 Mutlu, R.N., & Yazici, B. Copper-deposited aluminum anode for aluminum–air battery. Journal of Solid State Electrochemistry, 23, 529–541 (2019). https://doi.org/10.1007/s10008-018-4147-7.

11 Ma, J., Wen, J., Gao, J., et al. Performance of Al–0.5Mg–0.02Ga–0.1Sn–0.5Mn as anode for Al–air battery in NaCl solutions. Journal of Power Sources, 253, 419–423 (2014). https://doi.org/10.1016/j.jpowsour.2013.12.088.

12 Li, D., Liu, Y., Xie, Y., et al. Porous powder anode for high performance rechargeable aluminum batteries. Journal of Power Sources, 641, 236860 (2025). https://doi.org/10.1016/j.jpowsour.2025.236860.

13 Mori, R. Recent developments for aluminum–air batteries. Electrochemical Energy Reviews, 3, 344–369 (2020). https://doi.org/10.1007/s41918-020-00065-4.

14 Ma, Y., Sumboja, A., Zang, W., et al. Flexible and wearable all-solid-state Al–air battery based on iron carbide encapsulated in electrospun porous carbon nanofibers. ACS Applied Materials & Interfaces, 11, 1988–1995 (2019). https://doi.org/10.1021/acsami.8b15877.

15 Mohamed, S.G., Tsai, Y.Q., Chen, C.J., et al. Ternary spinel MCo2O4 (M = Mn, Fe, Ni, and Zn) porous nanorods as bifunctional cathode materials for lithium–O2 batteries. ACS Applied Materials & Interfaces, 7, 12038–12046 (2015). https://doi.org/10.1021/acsami.5b02601.

16 Niu, Q., Chen, B., Guo, J., et al. Flexible, porous, and metal–heteroatom-doped carbon nanofibers as efficient ORR electrocatalysts for Zn–air battery. Nano-Micro Letters, 11, 8 (2019). https://doi.org/10.1007/s40820-018-0231-0.

17 Liu, W., Placke, T., & Chau, K.T. Overview of batteries and battery management for electric vehicles. Energy Reports, 8, 4058–4084 (2022). https://doi.org/10.1016/j.egyr.2022.03.016.

18 Sun, Q., Dai, L., Luo, T., Wang, L., Liang, F., & Liu, S. Recent advances in solid-state metal–air batteries. Carbon Energy, 2022, 1–23. https://doi.org/10.1002/cey2.276.

19 Wang, Y., Sun, Y., Ren, W., Zhang, D., Yang, Y., Yang, J., Wang, J., Zeng, X., & NuLi, Y. Challenges and prospects of Mg–air batteries: A review. Energy Materials, 2, 200024 (2022). https://doi.org/10.20517/energymater.2022.20.

20 Wang, L., Snihirova, D., Deng, M., Vaghefinazari, B., Xu, W., Höche, D., Lamaka, S.V., & Zheludkevich, M.L. Sustainable aqueous metal–air batteries: An insight into electrolyte system. Energy Storage Materials, 52, 573–597 (2022). https://doi.org/10.1016/j.ensm.2022.08.032.

21 Li, J., Zhang, K., Wang, B., & Peng, H. Light-assisted metal–air batteries: Progress, challenges, and perspectives. Angewandte Chemie International Edition, 61, e202213026 (2022). https://doi.org/10.1002/anie.202213026.

22 Chantavas, A. Global market outlook for solar power. SolarPower Europe, 2022, 1–25. https://www.solarpowereurope.org/press-releases/world-installs-a-record-168-gw-of-solar-power-in-2021-enters-solar-terawatt-age.

23 Liu, Y., Lu, X., Lai, F., Liu, T., Shearing, P.R., Parkin, I.P., He, G., & Brett, D.J.L. Rechargeable aqueous Zn-based energy storage devices. Joule, 5, 2845–2903 (2021). https://doi.org/10.1016/j.joule.2021.10.011.

24 Murali, A.P., Duraisamy, S., Samuthiram, S., et al. Current and emerging methods for manufacturing of closed pore metal foams and its characteristics: A review. Journal of Materials Science, 60, 1187–1227 (2025). https://doi.org/10.1007/s10853-024-10318-y.

25 Mahto, R.P., Bhadauria, A., Bandhu, D., et al. A study on porosity and mechanical properties of the open aluminum metal foam through spark plasma sintering SDP technique. International Journal of Advanced Manufacturing Technology, 136, 4407–4417 (2025). https://doi.org/10.1007/s00170-025-15077-x.

26 Sun, S., Zhang, Z., Yan, L., et al. A novel superimposed porous copper/carbon film derived from polymer matrix as catalyst support for metal–air battery. Journal of Porous Materials, 29, 249–255 (2022). https://doi.org/10.1007/s10934-021-01163-4.

27 Jiao, X., Liu, Y., Cai, X., et al. Progress of porous Al-containing intermetallics fabricated by combustion synthesis reactions: A review. Journal of Materials Science, 56, 11605–11630 (2021). https://doi.org/10.1007/s10853-021-06035-5.

[1]Жукешов А.М.,
ф.-м.ғ.д., профессор, ORCID ID: 0000-0001-9153-323X,
e-mail: zhukeshov@physics.kz
[1]*Абдыбай Ұ.Б.,
докторант, ORCID ID: 0009-0002-5309-5827,
*e-mail: abdibay_ulan@mail.ru
[1]Салимов Е.Е.,
докторант, ORCID ID: 0009-0005-7712-6263,
e-mail: Salimov_ernar@mail.ru
[2]Карлос М.,
профессор, ORCID ID: 0000-0002-7374-505X,
e-mail: Carlos.meza@ieee.org

[1]Әл-Фараби атындағы Қазақ ұлттық университеті, Алматы қ., Қазақстан
[2]Анхальт қолданбалы ғылымдар университеті, Анхальт, Германия

ҚҰЙМА ЖӘНЕ КЕУЕКТІ ЭЛЕКТРОДТАРҒА НЕГІЗДЕЛГЕН МЕТАЛЛ-АУА БАТАРЕЯЛАРЫНЫҢ ӨНІМДІЛІК СИПАТТАМАЛАРЫНЫҢ САЛЫСТЫРМАЛЫ ТАЛДАУЫ

Аңдатпа

Қазіргі уақытта электр энергиясына деген өсіп келе жатқан сұранысты қанағаттандыруда электрохимиялық энергия сақтау жүйелерінің дамуы негізгі рөл атқарады. Жоғары меншікті энергия сыйымдылығына ие металл-ауа батареялары (МАБ) электр станцияларында резервтік қуат көздері ретінде пайдалануға перспективті шешімдердің бірі болып саналады. Оларды кеңінен енгізудегі негізгі шектеулердің бірі – анодтық материалдардың тиімділігін арттыру қажеттілігі. Бұл мақалада МАБ-тың жұмыс тиімділігін арттыру мақсатында кеуекті алюминий электродтарын қолдану ұсынылады. Әртүрлі технологиялар арқылы жасалған екі түрдегі кеуекті анодтар зерттелді. Ұнтақ алюминий анодында ток тығыздығы 20–30 мА/см^2 деңгейінде болып, монолитті (стандартты) анодтың көрсеткіштеріне сәйкес келді. Ал алюминий көбігі ток тығыздығының едәуір жоғары мәндерін – 52–64 мА/см^2 көрсетті. Кеуекті анодтардың қосымша артықшылығы – олардың салмағының 10–30%-ға аз болуы, бұл өз кезегінде МАБ-тың массалық-габариттік сипаттамаларын жақсартуға мүмкіндік береді және неғұрлым тиімді энергия жүйелерін құруға жол ашады.

Тірек сөздер: металл-ауа батареясы, алюминий аноды, кеуекті электрод, алюминий құймасы, электрохимиялық сипаттамалар, меншікті беткі аудан, энергия сақтау.

[1]Жукешов А.М.,
д.ф.-м.н., профессор, ORCID ID: 0000-0001-9153-323X,
e-mail: zhukeshov@physics.kz
[1]*Абдыбай У.Б.,
докторант, ORCID: 0009-0002-5309-5827,
*e-mail: abdibay_ulan@mail.ru
[1]Салимов Е.Е.,
докторант, ORCID: 0009-0005-7712-6263,
e-mail: Salimov_ernar@mail.ru
[2]Карлос М.,
профессор, ORCID ID: 0000-0002-7374-505X,
e-mail: Carlos.meza@ieee.org

[1]Казахский национальный университет им. аль-Фараби, г. Алматы, Казахстан
[2]Университет прикладных наук Анхальта, Анхальт, Германия

СРАВНИТЕЛЬНЫЕ ХАРАКТЕРИСТИКИ РАБОТЫ МЕТАЛЛ-ВОЗДУШНЫХ АККУМУЛЯТОРОВ С ЛИТЫМИ И ПОРИСТЫМИ ЭЛЕКТРОДАМИ

Аннотация

На сегодняшний день развитие электрохимических систем хранения энергии имеет важное значение для удовлетворения растущего спроса на электроэнергию. Металл-воздушные батареи (МАВ) из-за присущей им высокой энергоемкости являются перспективными устройствами для использования в энергетических установках как резервных источников. Проблема полноценного внедрения МАВ в эти системы упирается в решение вопроса об эффективных анодах. В настоящей работе предлагается использовать пористые материалы для увеличения эффективности работы МАВ. Пористые алюминиевые электроды двух типов с разной технологией изготовления были испытаны в качестве анодов для МАВ. Для анода из порошкового алюминия плотность тока составила (20–30) мА/см^2, что сравнимо с током для монолитного (стандартного) анода, но для пеноалюминия были получены более высокие значения плотности тока (52–64) мА/см^2. Так как масса пористых анодов будет на (10–30)% ниже, это является преимуществом в разработке новых типов МАВ с улучшенными массогабаритными показателями.

Ключевые слова: металл-воздушная батарея, алюминиевый анод, пористый электрод, алюминиевая пена, электрохимические характеристики, удельная поверхность, накопление энергии.

Article submission date: 12.09.2025